Proceedings of
The Fourth National Congress on Fluids Engineering
August 23-25, 2006, Kyungju, Korea

Flow Analysis around a Floating Cylinder in a Swirl Flow with a Stereoscopic-PIV

Doh, D.H.*, Hwang, T.G.** , Tanaka, K.*** and Takei, M.****

스테레오 PIV에 의한 원관내 선회유동중 실린더형 부유체 주위 유동 특성 해석

도덕희* · 황태규** · 다나카 코지*** · 타께이 마사****

Keywords *: Swirl Flow(선화유동), Floating Cylinder(부유체 실린더), Stereoscopic-PIV(스테레오PIV), LEDs, Conditional Sampling(조건부 샘플링)*

Abstract

The flow characteristics around a floating cylinder in a swirling flow field in a vertical pipe with a length of 600mm and an inner diameter of 100mm is investigated by the use of the Stereoscopic-PIV system. The measurement system consists of two cameras, a Nd-Yag laser and a host computer. Optical sensors(LEDs) were used to detect the location of the floating cylinder and to activate the Stereoscopic-PIV system. A conditional sampling Stereoscopic-PIV system was developed in which the flow fields around the floating cylinder are measured at the events of the activations. It has been verified that the motion of the floating cylinder becomes stable when the azimuthal velocity component of the swirl flow is maintained at stable states.

1. Introduction

Spiral swirl flows are widely used in the industries in which conveyance or transportation of solid particles such as cereals or chemical powders are needed since their flow characteristics have strong concentrations into the swirl axis, which makes the solid particles to be conveyed easily without producing big resistances with the pipe wall. In case of long distance conveyance of optical fibers or solid materials without contacting with the conveying pipes, stable controls on the spiral flows become important. The pneumatic transport of fragile and viscous materials is a big challenge in chemical and food industries; the problems of material breaking and sticking to the inner wall of pipeline. Currently the batch system has been used for handling these chemical materials, but the efficiency is too low. Many techniques have been employed to overcome these drawbacks of both pneumatic and batch systems, but none is completely satisfactory. The final goal of this work is to develop a high performance pneumatic transportation system for fragile and viscous materials. Horii used a spiral flow which has a steep axial velocity profile with swirling motion in order to transport particles without touching the inner wall, resulting in a high performance transporting system[1]. Tomita et al. used a swirling flow in order to control the particles' motion, but the particles touched to the inner wall of the conveying pipe [2]. To avoid the particles' touches onto the pipe wall, a forced vortex flow was introduced to the swirl flows. Many researches had been made on the flow itself but not on the flow around the conveyed material.

Takei et al.[3] showed that spiral flows maintain low velocity fluctuations and regular radial velocity component at the swirl center region. They investigated the velocity of conveyed ceramic balls using a laser doppler velocimetry and a stroboscope. Hui Li et al.[4] investigated the flow characteristics around the floating materials(polystyrene, polyethylene and vinyl) that are transported in a swirl and non-swirl flows. Tomita[5] used polyethylene spheres as conveyed materials in a swirl flow and reported the pressure drops in a horizontal pipe. Li and Tomida[6] carried out a numerical simulation on a strong swirl flow and non-swirl flow in a horizontal pipe. Experimental reports on the flow around a floating material in a swirl flow are very few.

The purpose of this study is to report the flow characteristics around a floating material in a vertical swirl flow using the Stereoscopic-PIV system, which provides valuable information for stable controls and for stable conveyances of the materials in the swirl flows.

2. Measurement System

2.1 Stereoscopic-PIV System

A hybrid stereoscopic-PIV system has been constructed to measure the swirl flows. For camera calibrations 10-parameter method [7] was used.

Since the arrangement of the cameras has a large view angle, the obtained images are strongly distorted, which makes the camera calibration so difficult. To overcome this matter, a two-dimensional image transformation on each camera image, warping, was carried out before using the original images for the camera calibration using the below Eq. (1). In this study, the image at the center physical plane (Z=0mm) was used to calculate the elements of the a_{ij} matrix.

* 한국해양대학교 기계정보공학부, doh@mail.hhu.ac.kr
** 한국해양대학교 산학협력단, andrew@bada.hhu.ac.kr
*** Okamoto Inc. Ltd., cpt.tanaka@imx.okamoto-inc.co.jp
**** Nihon Univ. Dept. of Mech. Eng., takei@mech.cst.nihon-u.ac.jp

$$x = \frac{a_{11}x_s + a_{12}y_s + a_{13}}{a_{31}x_s + a_{32}y_s + 1},$$
$$y = \frac{a_{21}x_s + a_{22}y_s + a_{23}}{a_{31}x_s + a_{32}y_s + 1} \quad (1)$$

x, y : coordinates before transformation
x_s, y_s : coordinates after transformation

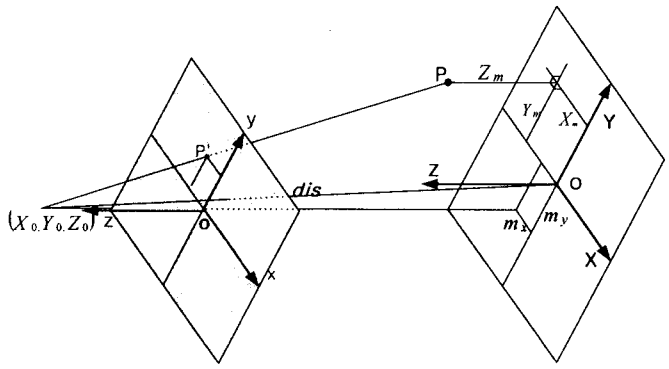

Fig. 1 The camera parameters on the absolute coordinate and the photographical coordinate

In the ten-parameter method, 10 parameters (6 exterior parameters: $dis, \alpha, \beta, \gamma, m_x, m_y$, 4 interior parameters: c_x, c_y, k_1, k_2) are obtained. (α, β, γ) represents the tilting angles of the axes of the photographic coordinates against the absolute axes. Fig. 1 shows a coordinate relation when the photographical axes had been set to parallel with the absolute coordinate by tilting with the angles (α, β, γ). (X, Y, Z) represents the absolute coordinate, and (x, y, z) the photographical coordinate of the image centroids of the targets and the seeded particles. The notation *dis* means the distance between the origin O(0, 0, 0) and the principal point (X_0, Y_0, Z_0) of the camera.
The coordinate (X_m, Y_m, Z_m) represents the position of the point P when the camera coordinate is rotated with the tilting angles to make the collinear set in one line as shown in Fig. 1. The m_x, m_y means the point at which the normal vector from the origin O(Xo, Yo, Zo) of the camera coordinate meets with the X-Y plane.
The collinear equation for every point between the two coordinates is expressed as Eq. (2). c_x and c_y are the focal distances for x and y components of the coordinate. Δx and Δy are the lens distortions as expressed as Eq. (3).

$$F = c_X \frac{X_m - m_x}{\sqrt{dis^2 - m_x^2 - m_y^2 - Z_m}} - (x - \Delta x) = 0,$$
$$G = c_y \frac{X_m - m_y}{\sqrt{dis^2 - m_x^2 - m_y^2 - Z_m}} - (y - \Delta y) = 0 \quad (2)$$

$$\Delta x = (x/r) \times \left(k_1 r^2 + k_2 r^4\right),$$
$$\Delta y = (x/r) \times \left(k_1 r^2 + k_2 r^4\right),$$
$$r = \sqrt{x^2 + y^2} \quad (3)$$

The three-dimensional positions of the vectors are expressed as Eq. (4).

$$\begin{bmatrix} X_P \\ Y_P \\ Z_P \end{bmatrix} = \frac{1}{2}\left\{ \begin{bmatrix} X_A \\ Y_A \\ Z_A \end{bmatrix} + \begin{bmatrix} X_B \\ Y_B \\ Z_B \end{bmatrix} \right\} \quad (4)$$

Here, X_A, Y_A and Z_A represent the absolute coordinates for camera A and X_B, Y_B and Z_B are for camera B. After obtaining the positions of the vector grid points (vector start points), the three-dimensional vector terminal points are calculated by combining the two-dimensional vector terminals of each camera's image. The two-dimensional vectors are obtained by the conventional gray level cross-correlation method[8].

2.2 Measurement Procedure

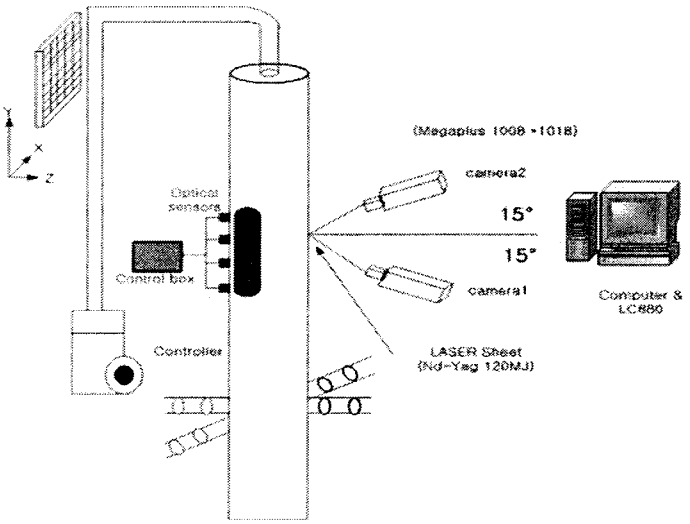

Fig. 2 Experiments with the Conditional Sampling Stereoscopic-PIV system

Fig. 2 shows the overall measurement system. Two digital cameras (Kodak ES1.0, 1k x 1k) were used for the stereoscopic measurements and arranged as seen in the figure. Smoke (Glycol , d=0.5~ 1μm)was used as seeding particles and it was let into the main pipe (D=110mm, L=600mm). Nd-Yag laser (120mJ, 15Hz) was used for flow field visualizations. The swirl flow is generated by suctioning the main pipe air at top with a blower. The air inlet is made at the bottom of the main pipe through four small horizontal pipes (d=10mm) as seen in the Fig. 2. A floating bar (d=12mm, h=60mm, polystyrene) was put into the swirl flow field in order to investigate the flow conditions at which its posture becomes upright rotating at a certain height from the bottom of the main pipe with stability. Its posture was sensed by the four optical sensors (LED, reflection type) attached on the pipe wall. When all of the sensors detected their signal reflected from the bar, which implies the posture of the floating bar is upright, a pulse signal is generated and it activates the stereoscopic PIV system. Measurements were carried out at two regions, 200mm~280mm and 400mm ~480mm from the bottom of the main pipe. That is, the measurements were made when the floating bar was at stable vertical position from the bottom. The positions of the bar were controlled by adjusting the suction power of the blower, 200rpm and 255rpm, at which the azimuthal velocity components measured at 40mm from the wall of the main pipe were 1.86m/sec and 2.47m/sec. These velocities are defined as Vs1 and Vs2 and

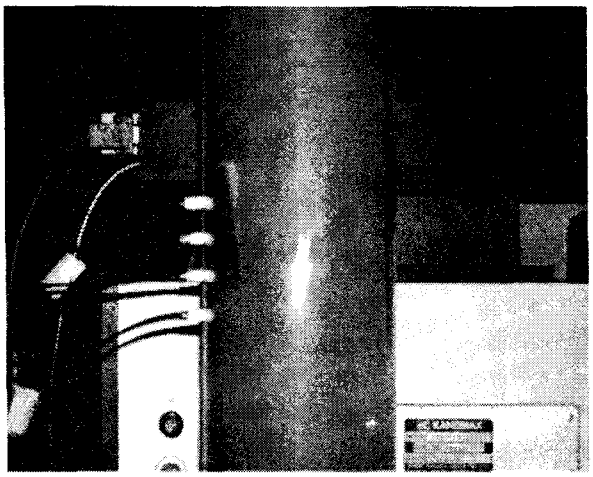

Fig. 3 Picture of experimentation

are used for normalization of the velocity vectors obtained by the stereoscopic PIV system. The images of the two cameras were captured in simultaneous through an image grabber installed on the host computer (2GHz).

Before commencing the main experiments the camera calibration was carried out. A flat plate (56mm x 48mm) was attached onto a traverse and was moved to several planes (-12mm, -8mm, -4mm, 0mm, 4mm, 8mm, 12mm) with 4mm distance at which the images of the plate were captured for camera calibration. Fig. 3 shows a picture taken at a instance when the bar maintains a stable rotation.

3. Measurement Results

Fig. 4 shows instantaneous raw images taken by the two cameras in Fig. 1. Fig. 5 shows an instantaneous three-dimensional vector distribution obtained by using the raw images. Fig. 6 shows the time-averaged vector distribution which was obtained by taking an average with 96 instantaneous raw vectors. Every instantaneous vector field was obtained at the time when the bar came into the same posture regions. That is, a conditional sampling for vector field was carried out and averaging was made at the same condition where the rotating bar comes into a certain area in the swirl flow.

The color legend means the w component of the three-dimensional vector field. Red means the plus direction (front direction) and blue means the minus direction (rear direction of the paper). It can be seen from the Fig. 6 that there exists a strong swirl in the main pipe. It can also be seen that there is upward flow near the bar and it seems to work as a lifting force on the floating bar.

Fig. 7 shows the mean velocity profiles at three different X-Z planes. The orthogonal coordinate was used to present the velocity vector components. The definition of the coordinate is shown in Fig. 6 and the three components of vectors were depicted as U, V and W. All components were non-dimensionalized. The W components in the outer region from the pipe center were bigger than those in the inner region while the U components showed reverse profile. Further, the magnitude of W component was much bigger than those of U and V components. It seemed that the W component plays an important role in stabilizing the posture of the floating bar while maintaining the same height of rotating location. It could be said from these figures that the bar's stable rotation at the same height along the outer region are not dependant on the magnitude of the swirl velocity but on the ratio of U, V and W component profiles.

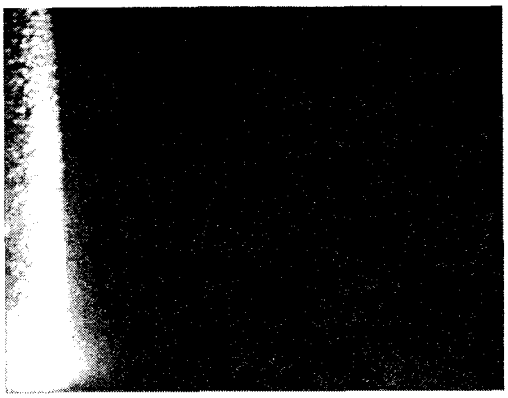

(by camera 1)

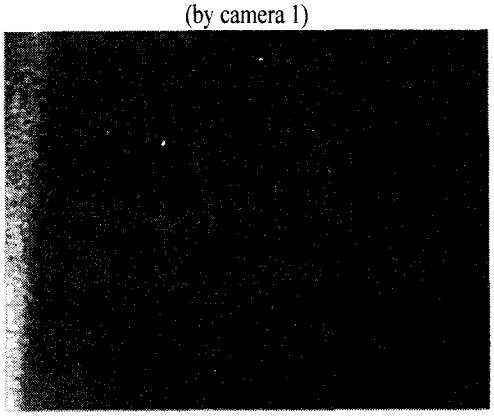

(by camera 2)

Fig. 4 Instantaneous raw images

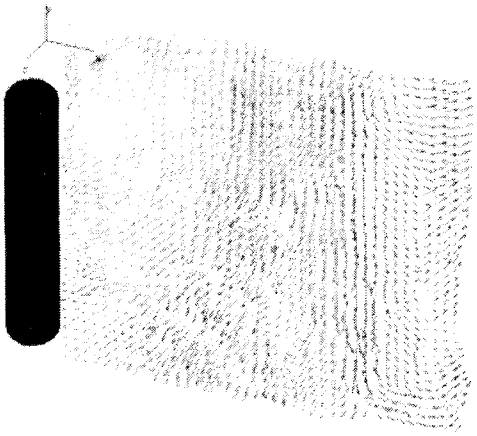

Fig. 5 Instantaneous 3D vector field

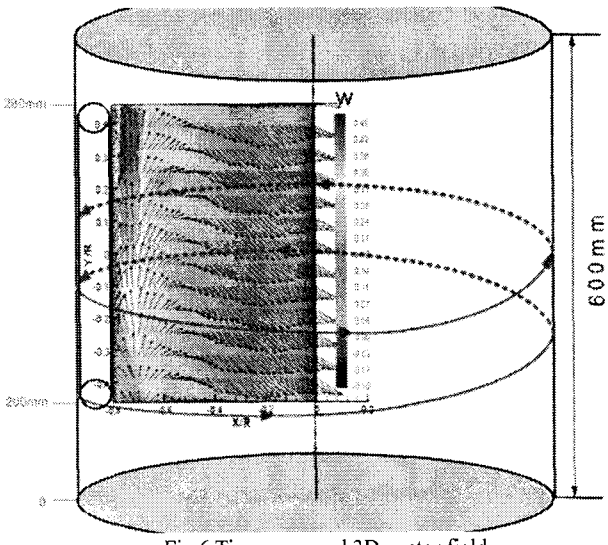

Fig.6 Time averaged 3D vector field

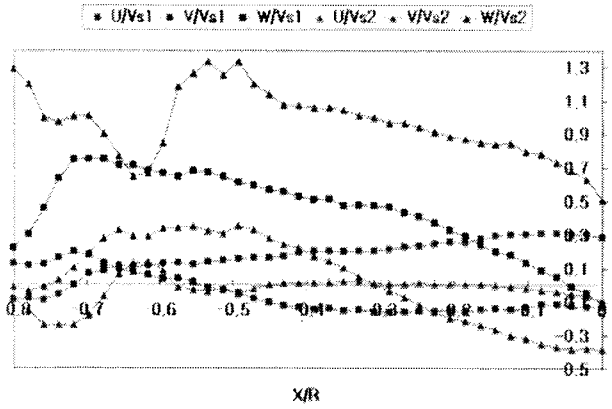

(a) Upper plane (Y/R=-0.32, Z/R=0)

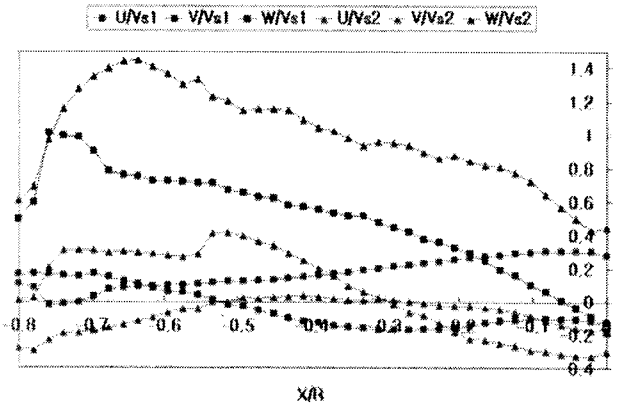

(b) Middle plane (Y/R=0.01, Z/R=0)

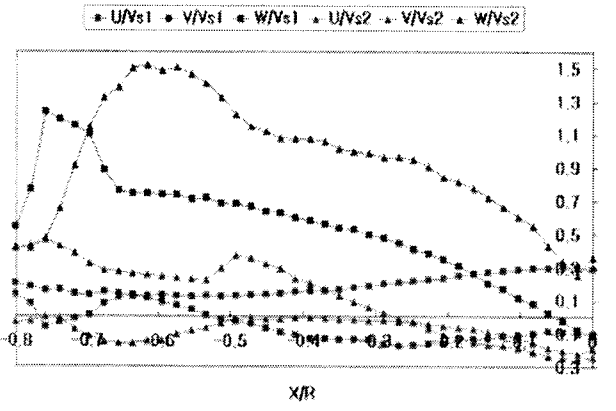

(c) Lower plane (Y/R=0.32, Z/R=0)

Fig. 7 Time-mean velocity fields

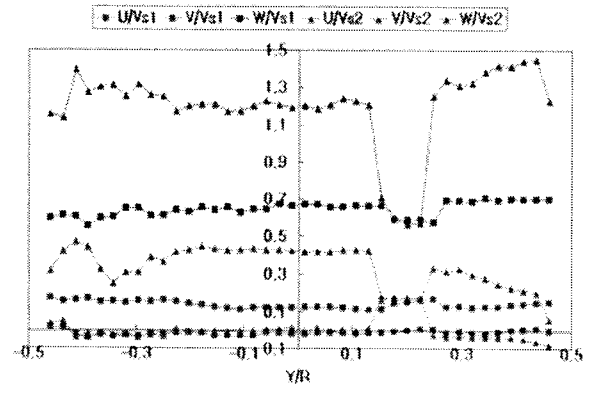

Fig. 8 Velocity profiles near the spiral zone (X/R=-0.51 & Z/R=0)

Fig. 8 shows the mean velocity profiles near the spiral zone. The spiral zone is defined at the place between the upward flow zone and the pure swirl zone as seen in Fig. 6(X/R= -0.4 ~ -0.5). This spiral flow seems to play a role of continuous rotation of the bar at a certain constant height. All three velocity components show constant magnitude ratio over the whole Y/R regions except the region Y/R=0.1~0.3, which may contribute the stable upright posture while rotating along the outer circle in the pipe. The large velocity deficit profile at Y/R=0.1~0.3 is due to the reflection effects of the surface of the main pipe. It can be said from this figure that the W component plays important role in making the posture of the floating bar upright with stable rotation along the circular orbital trajectory over the inner wall.

4. Conclusion

A Conditional Sampling Stereoscopic-PIV has been developed. The flow characteristic nearby the floating bar which is rotated by a swirl flow in a vertical pipe has been investigated by the use of the developed measurement system. W component played an important role in stabilizing the posture of the floating bar in upright maintaining the same orbital trajectory over the inner wall of the pipe. There was a spiral zone at X/R= -0.4 ~ -0.5 along the vertical line. This spiral flow seems to play a role in producing continuous rotations of the bar along the same orbital trajectory. It could be said that the bar's stable rotation at the same height along the same orbit is not dependant on the magnitude of the swirl velocity, but on the ratio of U, V and W component profiles. It could be said that the stable posture could be easily attained by maintaining the W component velocity stable.

Acknowledgements

This work was partly supported by the Korea Research Foundation Grant funded by the Korean Government ((KRF-2006-521-D00078).

References

[1] Horii K., 1990, "Experimental and theoretical study of turbulent swirling jets issuing from a round orifice", Israel J. Technology, Vol. 4, pp. 44-54.

[2] Tomita Y., 1996, "An Experimental Study of Swirling Flow Pneumatic Conveying System in a Horizontal Pipeline", ASME Fluid Engineering, Vol. 118, No.3, pp.526-530.

[3] Takei M., 1997, "Transporting particles without touching pipe wall", Proc. of ASME Fluids Engineering Div. Summer Meeting, pp.1-5.

[4] Li H., 1994, "Research of swirling flow pneumatic conveying system in a vertical pipeline(Coefficients of Power Consumption and Additional Pressure Drop)", JSME, Vol. 66, pp.571-580.

[5] Tomita, Y., 1993, "Research of swirling flow pneumatic conveying system in a hrizontal pipeline (Particle Velocity and Concentration Profiles)", JSME, Vol. 59, pp.558-568.

[6] Li, H., Tomita, Y., 1994, "A numerical simulation of swirling flow pneumatic conveying in a horizontal pipeline", JSME., Vol. 60, pp.575-584.

[7] Doh, D.H., Hwang, T.G., Saga, T., 2004, "3D-PTV measurements of the wake of a sphere", Measurement Science and Technology, Vol. 15, No. 6, pp.1059-1066.

[8] Kimura, I., Takamori, T. and Inoue, T., Image processing instrumentation of flow by using correlation technique, Flow Visualization, Vol. 6, No.22, (1986), pp.105-108.